

## THE MULTI-METEOROLOGY AIR QUALITY (MMAQ) ENSEMBLE PROJECT: VARIANCE GENERATED BY A WRF VARIED PHYSICS ENSEMBLE

Debra Baker\* and Eugenia Kalnay

Department of Atmospheric and Oceanic Sciences, University of Maryland, College Park, MD, USA

### 1. INTRODUCTION

The Multi-Meteorology Air Quality (MMAQ) Ensemble Project applies the ensemble forecasting techniques that have so successfully improved numerical weather prediction [Kalnay, 2003] to regional air quality forecasting. The ensemble focuses on meteorological uncertainty, the largest source of error in air quality modeling [McKeen et al., 2005]. The models chosen for this project are WRF-ARW (Weather Research and Forecasting model—Advanced Research WRF), SMOKE (Sparse Matrix Operator Kernel Emission system), and CMAQ (Community Multiscale Air Quality model). The project uses varied physics mesoscale meteorology ensembles to create emissions ensembles. Both sets of ensembles are used to initialize and generate air quality ensembles. The ozone forecasts for each ensemble and the ensemble average will then be evaluated against observations.

The research questions that will be addressed are (1) How sensitive is emissions model to meteorology physics options? (2) How sensitive is air quality model to meteorology physics options? (3) Is the ensemble spread sufficient to represent forecast uncertainty?

This paper will examine the preliminary results of MMAQ. It focuses on the spread generated by the WRF varied physics ensemble in meteorology variables essential to air quality modeling.

### 2. METHODOLOGY

The WRF-ARW v. 2.2.1 mesoscale meteorology model used for MMAQ is a fully compressible, nonhydrostatic model with an Eulerian mass dynamical core [Skamarock et al., 2005]. Unlike MM5 (5th-Generation NCAR/Penn State Mesoscale Model), mass is conserved so that WRF can be better coupled with chemistry/air quality models. WRF can easily generate varied physics ensembles. It includes multiple physics options for turbulence/diffusion, radiation (long and

shortwave), land surface, surface layer, planetary boundary layer, cumulus, and microphysics. Both CMAQ and WRF use Arakawa C grid staggering and the mass conserving vertical coordinate is compatible with the generalized vertical coordinates of CMAQ, which reduces interpolation error [Byun and Schere, 2006].

In the MMAQ project, WRF is initialized with high resolution (5 m) static data for topography, land use, and soil types for the bottom and top layers. All dynamic fields are initialized using NAM (North American Mesoscale) model output at 40 km resolution and boundary conditions are updated every 3 hours.

The domain for the MMAQ ensembles is the continental United States (CONUS) with 12 km resolution. The domain has 30 uneven levels, giving 29 layers, with higher resolution in the planetary boundary layer (PBL). The middle of the lowest layer is defined at an altitude of approximately 10 m, the level at which surface winds are typically measured.

The case study selected to test the MMAQ ensembles is the ozone event on 2008 June 12 to 13. This event generated red code days in the Northeast, Midwest, and West Coast United States. It also features transport of ozone east from June 12 to June 13. By using the MMAQ ensemble, we can determine whether it would have been able to improve the forecast, e.g., have forecast red code days in the areas in which they occurred but were not forecast.

### 3. WRF VARIED PHYSICS ENSEMBLES

The meteorology ensembles are created through using different combinations of three physics options: land surface model, planetary boundary layer (PBL) and surface layer (SL) schemes, and cumulus-convection parameterizations. Selecting two options for each type of physics results in eight ensemble members.

The two land surface models used are *Noah Land Surface Model* [Ek et al., 2003] and the *Rapid Update Cycle (RUC) Land Surface Model* [Benjamin et al., 2004]. Both are sophisticated land surface models that include vegetation and

---

\*Corresponding author: Debra Baker, Department of Atmospheric and Oceanic Sciences, University of Maryland, College Park, MD 20742; e-mail: drb@atmos.umd.edu

canopy water effects, frozen soil physics, and fractional snow cover. The most significant difference in the two models is how they discretize the soil below the surface. The Noah Land Surface Model has four layers below ground: 0-10 cm, 10-40 cm, 40-100 cm, and 100-200 cm. The RUC Land Surface Model uses six levels: 0 cm, 5 cm, 20 cm, 40 cm, 160 cm, and 300cm. Unlike Noah, RUC has multi-layer snow with varying snow density and temperatures. RUC relies on internal values and does not use other properties or tables from USGS that Noah does.

The two PBL options used the *Mellor-Yamada-Janjić (MYJ) PBL Scheme* [Mellor and Yamada, 1982; Janjić, 2001] and *Yonsei University PBL Scheme* [Hong et al., 2003]. MYJ uses a 1.5 order, level 2.5 turbulence closure approach. It predicts turbulent kinetic energy (TKE) from which it calculates diffusivity (K) and PBL height. It is a local vertical mixing scheme in the boundary layer and free atmosphere. An upper limit is placed on the master scale length. Entrainment is parameterized, not explicit. It is known to have a moist, cool bias. The Yonsei University scheme is a non-local K scheme with explicit entrainment. It uses a K profile and a countergradient term for heat and moisture in an unstable boundary layer. PBL height is calculated from the buoyancy/thermal profile. Vertical diffusion in the free atmosphere is based on the Richardson number.

The two PBL schemes have complementary surface layer schemes: *the Eta Janjić similarity surface layer scheme* [Janjić, 2001] for MYJ PBL scheme and the *MRF (Medium Range Forecast) surface layer scheme* [Chen et al., 1997] for the Yonsei University PBL scheme. Both surface layer schemes are based on similarity theory. Eta Janjić incorporates a viscous sublayer that is implicitly parameterized through roughness height for land and explicitly parameterized for water. In contrast, MRF uses a parameterized relationship between roughness length and friction velocity for water surfaces. Eta Janjić is able to simulate unstable surface layers with minimal wind speeds, a situation that can produce singularities in other surface layer schemes. An iterative method is used to compute heat, moisture, and momentum fluxes. The MRF surface layer scheme (also known as the first Monin-Obukhov similarity scheme) uses stability functions based on four stability regimes: stable, neutral, forced convection, and free convection [Zhang and Anthes, 1982]. The heat and moisture exchange coefficients are enlarged using the concept of “convective velocity.”

The two convection parameterizations are the modified version of the *Kain-Fritsch (KF-Eta) cumulus scheme* [Kain, 2004] and the *Grell-Dévényi Ensemble (GDE) cumulus scheme* [Grell and Dévényi, 2002]. KF-Eta is a relatively simple model of cumulus cloud development and precipitation with a long history of development behind it. GDE is a newer cloud scheme that utilizes an unweighted ensemble average of 144 members and is adapted from data assimilation techniques. KF Eta applies a mass flux approach to updrafts and downdrafts, while GDE explicitly simulates them. In GDE, the downdrafts are linked to shear so that more shear results in less precipitation. Both cumulus parameterizations model cloud entrainment and detrainment. In KF Eta, the entrainment rate is calculated from the low level convergence. A minimum entrainment rate avoids singularities in unstable and dry conditions. GDE ties the strength of convection to the large scale so that stabilization by convection results in destabilization. The ensemble approach allows GDE to use multiple closure assumptions, which include convective available potential energy (CAPE) removal, low-level vertical velocity, quasi-equilibrium, or moisture convergence.

The MMAQ ensemble combinations are summarized in Table 1.

Table 1: WRF Varied Physics Ensembles

Ensemble	Land	PBL/SL	Cumulus
1	Noah	MYJ	KF-Eta
2	Noah	MYJ	GDE
3	Noah	Yonsei	KF-Eta
4	Noah	Yonsei	GDE
5	RUC	MYJ	KF-Eta
6	RUC	MYJ	GDE
7	RUC	Yonsei	KF-Eat
8	RUC	Yonsei	GDE

The WRF ensembles share the same settings for the other key physics options. These are the CAM (Community Atmosphere Model) shortwave and longwave radiation, Thompson microphysics, Coordinate Surface/Simple diffusion, and Smagorinsky 2D Deformation turbulence parameterizations. The simulation time step is set for 30 seconds to avoid Courant-Friedrichs-Lewy (CFL) violations. The PBL and surface layer schemes are run every time step but the cumulus parameterization is called every 2 minutes. The radiation parameterization is only run every 12 minutes. WRF is set to zero out very small and negative microphysics cloud and precipitation variables as well as negative water vapor

variables if they fall below a critical value. All CAM and GDE options are set to the default values, except that the CAM absolute dimension 2 is set to the number of vertical layers in the grid (29). The number of soil layers is changed from 4 for Noah to 6 for RUC. Vertical velocity damping is enabled and the model is run in a non-hydrostatic mode. A positive definite advection scheme is used for moisture, which enhances summer precipitation simulations. The output is produced hourly.

#### 4. WRF ENSEMBLE VARIANCE

The WRF ensemble results were analyzed to determine the amount of spread in the ensemble for meteorology variables most important to air quality: 2 m temperature, 10 m U and V winds, 2 m water vapor mixing ratio, and accumulated cumulus precipitation [Seaman, 2000].

Since the timing and location of the variance in meteorology factors is essential given the diurnal variability in ozone production, an hour-by-hour anomaly was calculated for each grid box using an unweighted ensemble average as the mean. From the anomalies, an average variance for all eight ensembles was calculated. To evaluate the impact of the six different parameterizations used, an average variance for the four ensembles using each scheme was also computed.

##### 4.1 Temperature at 2 m

The value of 2 m temperature (T2) over the simulation period and domain ranged from 266 K to 315 K in the ensemble average. Temperature peaks occurred at 2:00 pm EST. Looking at the variance for all ensembles, the largest variance in 2 m temperature occurs at night from 8:00 p.m. to 5:00 a.m. EST. The peak variance values occurs at 8:00 p.m. EST and forms a band from Maine to Louisiana and from Montana to Utah, with some values of 25 K<sup>2</sup> (see Figure 1). During the daylight hours, the variance reaches only 5 K<sup>2</sup> and only in isolated areas of the continental United States.

The two land surface models show the same diurnal and geographical patterns but Noah model has the larger magnitude of variance, with a difference of up to 14 K<sup>2</sup> in maximum variance. The two PBL schemes have similar magnitude variance but the 2 m temperature variance in Mellor-Yamada-Janjić is more prevalent in the eastern U.S. and in the Yonsei University is more prevalent in the western U.S. The two cumulus

schemes have 2 m temperature variance very similar to the variance of all ensembles.

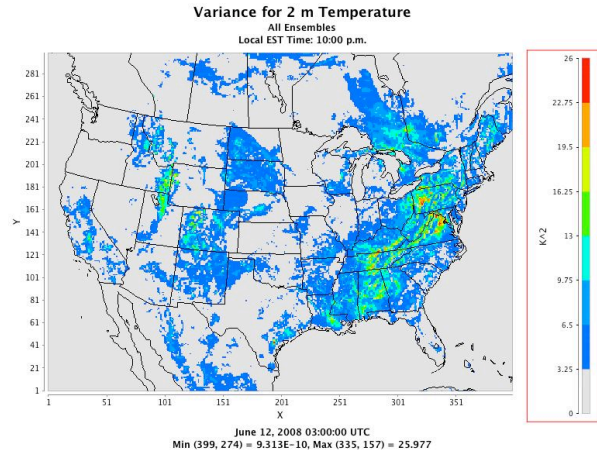


Figure 1: Peak hourly variance of 2 m temperature for all ensembles.

##### 4.2 U Winds at 10 m

The values of 10 m x-coordinate wind (U10) over the simulation period and domain ranged from -13 to 15 m/s in the ensemble average. The highest values are in the early evening of June 13. Looking at all ensembles, variance appears to average below 1 m<sup>2</sup>s<sup>-2</sup>. Higher values appear to be isolated from Nebraska to Texas and near Florida (see Figure 2).

The variance in the two land surface models is very similar in spatial distribution and magnitude. However, the Yonsei University PBL scheme shows higher magnitude U wind variance than the Mellor-Yamada-Janjić PBL scheme. The two cumulus schemes showed very little divergence in variance between each other and with all ensembles.

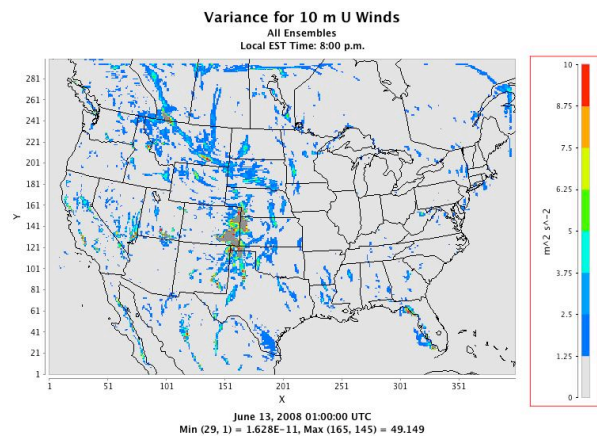


Figure 2: Peak hourly variance of 10 m U wind for all

ensembles.

### 4.3 V Winds at 10 m

The range of 10 m y-coordinate wind (V10) over the simulation period ranged from -17 to 13 m/s in the ensemble average. Like U winds, the highest variances for all ensembles are in the evening. Again, the average variance appears to be below  $1 \text{ m}^2\text{s}^{-2}$ . The peak variance in V winds occurs at 5:00 p.m. EST and is concentrated over Iowa (see Figure 3).

Overall, there is not much difference in magnitude of variance between the two land surface models. However, the Noah Land Surface Model shows more variance in the eastern United States than the RUC Land Surface Model. The same pattern occurs with the two PBL schemes: the Yonsei University parameterization has more variance in the eastern U.S. than the Mellor-Yamada-Janjić scheme. No significant contrast could be found for the two cumulus parameterizations.

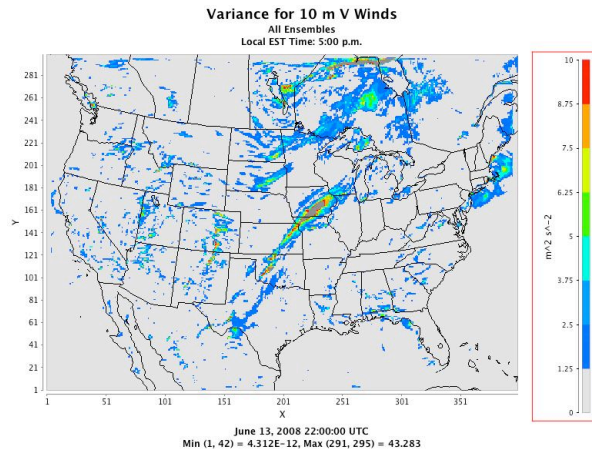


Figure 3: Peak hourly variance of 10 m V wind for all ensembles.

### 4.4 Water Vapor Mixing Ratio at 2 m

The value of 2 m water vapor mixing ratio (Q2) over the simulation period ranged from 0 to  $1.6 \times 10^{-2} \text{ kg/kg}$  in the ensemble average. It grows to larger values as the episode proceeds, showing a large swirling pattern from the Atlantic Ocean off the Northeast U.S. traveling southwest and turning around Florida until it is northeast from Arkansas to New York State. This may be due to model spin-up since the NAM humidity data was not used to initialize it. Another WRF run with a modified

Vtable that will incorporate this data is planned. The variance for water vapor for all is highest in magnitude at 3:00 p.m. and is focused in the Midwest, South, and all along the East Coast (see Figure 4).

This variance is contributed primarily by the RUC Land Surface Model, which has a significantly stronger variance compared to the Noah Land Surface Model ensembles. The Mellor-Yamada-Janjić PBL scheme contributes the majority of the variance from Louisiana up to Michigan while its variance in other parts of the United States is similar in location and magnitude to the Yonsei University PBL scheme. The two cumulus parameterizations show few differences in water vapor variances from all ensembles.

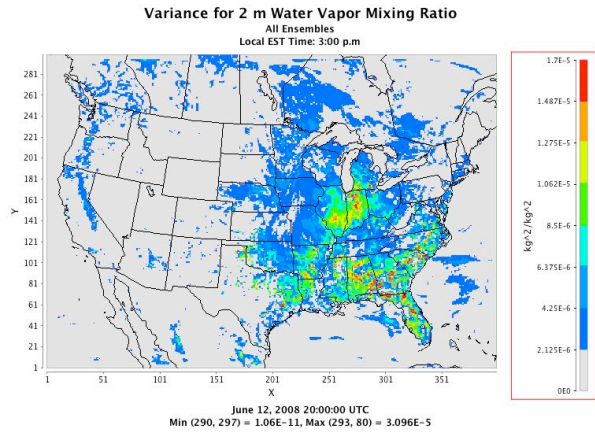


Figure 4: Peak hourly variance of 2 m water vapor mixing ratio for all ensembles.

### 4.5 Accumulated Cumulus Precipitation

The values for accumulated total precipitation from cumulus clouds (RAINNC) in the ensemble average ranges up to 20 mm during the entire simulation period. There was a significant line of thunderstorms from Kansas north to Wisconsin in the night at the end of the simulation period. The variance for all ensembles for this rain event reaches up to almost  $400 \text{ mm}^2$ , indicating a standard deviation almost equal to the average total convective rainfall (see Figure 5).

Although the land surface models have a similar magnitude of variance, the choice of land surface option does have a significant impact on convective rainfall. The RUC Land Surface Model ensembles have a larger area of variance compared to the Noah Land Surface Model as well as two additional storms north of the main line of thunderstorm. In contrast, the two PBL schemes have similar areas of variance in accumulated



convective rainfall but Mellor-Yamada-Janjić has a significantly higher magnitude of variance than Yonsei University PBL schemes.

Not surprisingly, the cumulus parameterizations show the largest divergence in maximum variance over the simulation period. The magnitude and area of variance are larger for the Grell-Dévényi Ensemble compared to the Kain-Fritsch cumulus parameterization. The two northern storm systems only appear in the Grell-Dévényi Ensemble scheme. In addition, the convective rainfall event in the Grell-Dévényi Ensemble scheme starts two hours earlier. The convective rain event continues beyond the end of the simulation period, so any difference in the time the storms would be predicted to end by the two cumulus schemes cannot be ascertained.

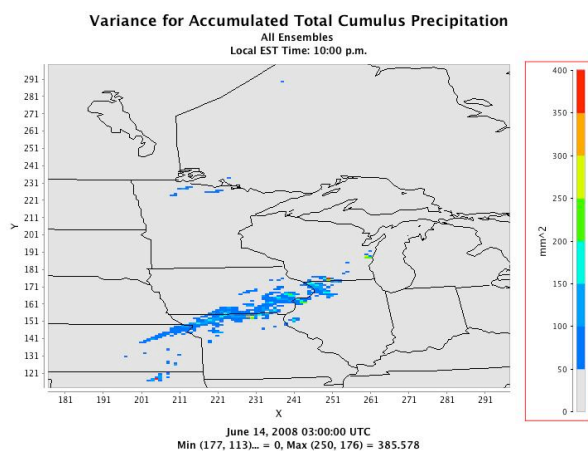


Figure 5: Peak hourly variance of accumulated total cumulus precipitation for all ensembles (portion of the domain with relevant data has been magnified).

The accumulated total non-cumulus precipitation was minimal with a maximum value of 1.3 mm. The nonconvective storms occur west of California and above Michigan near the end of the simulation period. These all occur near boundaries of the simulation, which makes the results less reliable.

## 5. DISCUSSION

The magnitude and area of the variance generated by the WRF varied physics ensemble in key meteorological variables is significant. It shows good potential for capturing some of the meteorology uncertainty in ozone forecasting. One barrier will be the timing of the maximum variance. For all but the water vapor mixing ratio, the peak variance occurs in the evening and night so its direct impact on ozone production forecasts may

be minimal. However, nocturnal ozone forecasts have accuracy problems [Delle Monache et al., 2006] on which this WRF ensemble may be able to shed some light.

Another potential problem is that the location of high variance does not occur near the high ozone areas for convective and nonconvective precipitation and only marginally for wind variance. This is not surprising given that ozone events are correlated with low winds and stagnant conditions. However, the temperature and moisture have high variance in ozone-related locations.

Other relevant meteorology variables known to play a major role in air quality simulations have not yet been analyzed, including PBL height (PBLH), surface emissivity (EMISS), friction velocity (UST), time-varying roughness length (ZNT), heat flux (HFX), ground heat flux (GRDFLX), latent heat flux (LH), and moisture flux (QFX). These factors may increase the spread of the emissions and air quality ensembles.

## 6. FUTURE WORK

The eight MMAQ WRF ensembles and ensemble average analyzed above are now ready to be processed by the Meteorology-Chemistry Interface Processor (MCIP). This output will be used in the SMOKE model to generate meteorology-dependent emissions including point, mobile, and biogenic sources. The sensitivity of these emissions to the meteorology variances will then be analyzed. Each WRF ensemble member and its complementary SMOKE ensemble member will be used to generate one CMAQ ensemble. The sensitivity of ozone predictions to meteorology variance will then be assessed.

## ACKNOWLEDGMENTS

Debra Baker was supported by the NSF Graduate Fellowship Program and this research was carried out in partial fulfillment of her University of Maryland doctoral requirements. The authors would like to thank Pius Lee, Jeff McQueen, Russ Dickerson, Da-Lin Zhang, Ross Salawitch, and Jeff Stehr for their help. No three-model ensemble can be run without a great deal of technical help. We are especially grateful to Doug Baker, Scott Spak, Robert Fovell, Carlie Coats, Chanh Kieu, Patricia Castellanos, Chris Lougher, Scott Rabenhorst, David Kuhl, Elizabeth Satterfield, Kaitlin Littlefield, Tanya Otte, Zac Adelman, Neil Davis, Liz Smith, Patricia Miller, Mike Barth, and wrfhelp as well as the following web forums and listservs: WRF, Models-3, EM

Regional, Mac Unix Porting, Mac SciTech, ifort, netCDF, NCO, fink, and CPAN.

Cambridge University Press, Cambridge, 2003, 341 pp.

## REFERENCES

- Benjamin, S. G., G. A. Grell, J. M. Brown, and T. G. Smirnova, Mesoscale weather prediction with RUC hybrid isentropic-terrain-following coordinate model, *Mon. Wea. Rev.*, **132**, 473-494, 2004.
- Byun, D. W., and K. L. Schere, Review of the governing equations, computational algorithms, and other components of the Models-3 Community Multiscale Air Quality (CMAQ) modeling system, *Appl. Mechanics Rev.*, **59**, 51-77, 2006.
- Chen, F., Z. Janjić, and K. Mitchell, Impact of atmospheric surface-layer parameterizations in the new land-surface scheme of the NCEP mesoscale Eta model, *Bound.-Layer Meteor.*, **85**, 391-421, 1997.
- Delle Monache, L., T. Nipen, X. Deng, Y. Zhou, and R. B. Stull, Ozone ensemble forecasts: 1. A Kalman filter predictor bias correction, *Geophys. Res. Lett.*, **111**, D05308, 2006.
- Ek, M. B., K. E. Mitchell, Y. Lin, E. Rogers, P. Grunman, V. Koren, G. Gayno, and J. D. Tarpley, Implementation of Noah land surface model advances in the National Centers for Environmental Prediction operational mesoscale Eta model, *J. Geophys. Res.*, **108** (D22), 8851, 2003.
- Grell, G. A., and D. Dévényi, A generalized approach to parameterizing convection combining ensemble and data assimilation techniques, *Geophys. Res. Lett.*, **29**, 1693, 2002.
- Hong, S.-Y., J. Dudhia, and Y. Noh, A new vertical diffusion package with explicit treatment of entrainment processes, Proceedings of the International Workshop on NWP Models for Heavy Precipitation in Asia and Pacific Areas, Japan Meteorological Agency, Tokyo, Japan, 2003.
- Janjić, Z., *Nonsingular Implementation of the Mellor-Yamada Level 2.5 Scheme in the NCEP Meso Model*, NCEP Office Note, #437, 2001, 61 pp.
- Kain, J. S., The Kain-Fritsch convective parameterization: An update, *J. Appl. Meteor.*, **43**, 170-181, 2004.
- Kalnay, E., *Atmospheric Modeling, Data Assimilation, and Predictability*, Cambridge University Press, Cambridge, 2003, 341 pp.
- McKeen, S., J. Wilczak, G. Grell, L. Djalalova, S. Peckham, E.-Y. Hsie, W. Gong, V. Bouchet, S. Menard, R. Moffet, J. McHenry, J. T. McQueen, Y. Tang, G. R. Carmichael, M. Pagowski, A. Chan, T. S. Dye, G. Frost, P. C. Lee, and R. Mathur, Assessment of an ensemble of seven real-time ozone forecasts over eastern North America during the summer of 2004, *J. Geophys. Res.*, **110**, D21307, 2005.
- Mellor, G. L., and T. Yamada, Development of a turbulent closure model for geophysical fluid problems, *Rev. Geophys. Space Phys.*, **20**, 851-875, 1982.
- Seaman, N. L., Meteorological modeling for air-quality assessments, *Atmos. Environ*, **34**, 2231-2259, 2000.
- Skamarock, W. C., J. B. Klemp, J. Dudhia, D. O. Gill, D. M. Barker, W. Wang, and J. G. Powers, *A Description of the Advanced Research WRF Verion 2, Mesoscale and Microscale Meteorology Division*, National Center for Atmospheric Research, Boulder, Colorado, 2005, 88 pp
- Zhang, D., and R. A. Anthes, A high-resolution model of the planetary boundary layer--sensitivity tests and comparison with SESAME-79 data, *J. Appl. Meteor.*, **21**, 1594-1609, 1982.